Stability of Thin-Walled Steel Elements of Composite Steel and Concrete Structures

Yurii Avramenko, Alina Zyhun, Samira Akbarova, and Oleg Yurin

Abstract This paper investigates the behavior of new type of steel and concrete composite structures. With a view of a more effective use of CFS in modern construction (increasing the carrying capacity while reducing the thermal conductivity) the authors propose to fill the open cavities of thin-walled steel structures with light insulating concrete to create ultralight steel and concrete composite elements. The paper presents the results of a theoretical analysis of the local stability of thin-walled steel elements supported by lightweight concrete. The study of the influence of structural parameters on the local stability of steel elements of reinforced concrete structures. The comparison of experimental results with the results of calculations is performed in accordance with the theory of elasticity and the proposed method.

Keywords Local stability · Cold-formed structures · Composite steel and concrete structures · Plates · Finite element

1 Introduction

Over the past couple of decades, constructions using steel thin-walled cold-formed profiles (cold-formed structures—CFS) [2, 4], also known as LiteSteel structures, are becoming more common in buildings.

Among the most common types of cross-sections of cold-formed profiles, should be allocated the C-sections used primarily as load-bearing structures of ceilings and walls of low-rise buildings, as well as Z-shaped (Z-profiles), the scope of which are purlins and wall coverings (see Fig. 1).

In general, the use of CFS in the load-bearing structures has a number of features caused primarily by their thickness and specific forms of section. Consequently, a

Y. Avramenko (✉) · A. Zyhun · O. Yurin
National University «Yuri Kondratyuk Poltava Polytechnic», Pershotravnevyj Ave. 24., Poltava 36011, Ukraine

S. Akbarova
Azerbaijan University of Architecture and Construction, Ayna Sultanova 11, Baku, Azerbaijan

V. Onyshchenko et al. (eds.), *Proceedings of the 3rd International Conference on Building Innovations*, Lecture Notes in Civil Engineering 181,
https://doi.org/10.1007/978-3-030-85043-2_1

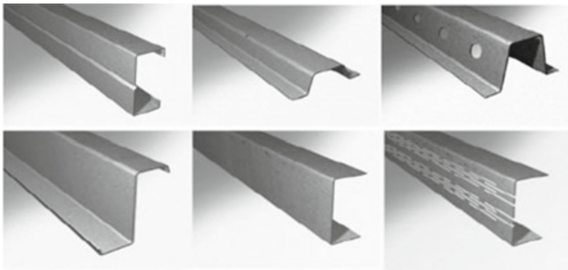

Fig. 1 Example of structures failures as local buckling of CFS members

Fig. 2 Example of structures failures as local buckling of CFS members

significant feature of this type of elements is their possibility of local buckling of flanges and walls under bending due to axial compression; the bending torsion owing to the behavior of flexural and compressed members with eccentricities; significant thermal conductivity of solid profiles, which leads to forming of heat-conducting inclusions etc.

For the most structures under operating conditions, local loss of stability is unacceptable and can be the cause of structures failures, as shown in Fig. 2.

Structural failure is the value of critical stresses caused by local bending of steel thin-walled cold-formed elements (plates) of lightweight composite steel and concrete structures.

In this respect, one of the ways to increase the carrying capacity of this type of structural elements can be to fill them with an ultralight weight concrete. In this case, the complex structure formed in this manner allows using the advantages of each of the components in the most efficient way by combining a carrier and heat-insulating functions.

Thus, the main objectives of these investigations are theoretical and experimental validation of CFS using efficiency combined with ultralight weight concrete (ultra-light steel and concrete composite structures) in order to increase the local stability of thin-walled steel profiles under complex types of deformation.

The authors suggest to fill the open cavities of thin-walled steel structures with light insulating concrete to create ultralight steel and concrete composite elements for a more effective using of CFS in modern construction (increasing the carrying capacity while reducing the thermal conductivity).

2 Methods of Study

The investigation approach used in this study, develops a numerical model to represent a behavior of ultralight steel and concrete composite structures (USCCS) under loading. The intended outcome of this modeling effort and experimental investigations was to establish a fundamental understanding of the local stability of CFS that is supported by concrete filling. The numerical modeling was used to confirm the existing, experimental data which are limited, on the behavior and ultimate capacity of light steel–concrete composite structures.

Experimental studies were conducted to verify the proposed approach, in which quantitative and qualitative data. It was the data about obtaining of the influence of steel elements thickness and concrete composition of reinforced concrete structures on local stability and stress–strain state of compressed steel and reinforced concrete structures under static load and their bearing capacity and the nature of the destruction. For example, there are concrete cubes 100 × 100 × 100 mm, which are supported on both sides by steel plates, 1 mm thick.

Separate plates (compartments) of steel structural elements are calculated and simplifications are introduced, which consist in the improvement of conditions of plate edges fixing and contour loads are introduced into the schematization. Freely supported plates are considered in most available studies and freely supported contour is provided in practical calculations. Actual fastening conditions can occupy any intermediate position between free support and fixed support, but the difference in the magnitude of the critical load can be quite significant.

The commercial finite element (FE) computer package [1, 8] was used to generate the numerical models. The accuracy and validity of the FE simulation and analysis were investigated through comparison of the experimental data and the results of theoretical analysis.

3 Materials Properties

The authors suggest to use the ultralight weigh concrete such a polystyrene concrete to fill the open cavities of thin-walled steel structures. Expanded polystyrene concrete is an especially lightweight (ultra-light) concrete with a cementing agent and a porous aggregate, such as expanded polystyrene aggregate, which can be used as an insulating and structural material.

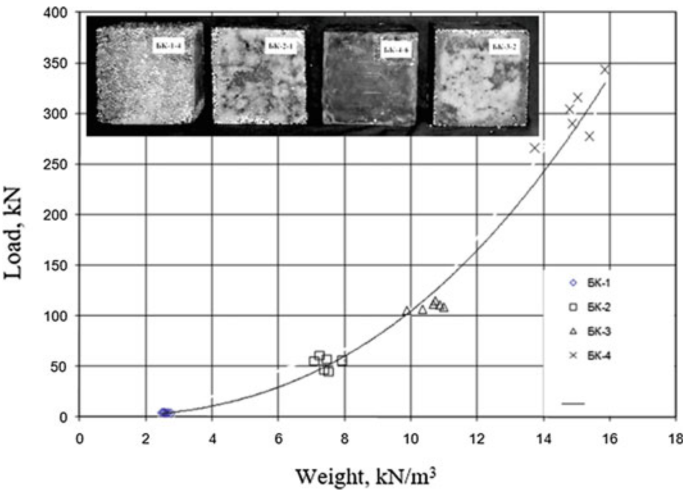

Fig. 3 The initial stress state of the plate on an elastic basis

In this regard, polystyrene concrete is mostly used for building envelopes of framed structures with a different number of floors, in facade systems, as heat and sound insulation [5–7, 9, 10, 12–16] between floors and roofing, etc.

It is obvious that the strength and deformation properties of polystyrene concrete largely depend on its composition, specifically depending in particular the water-cement ratio and the percentage of porous aggregate and cement. Therefore, the specific weight and strength of materials are functionally related [11].

Figures 3 shows the received experimetal relationship between specific weight and strength of standard concrete cubes with polystyrene concrete with different compositions.

Thus, the analysis of experimental results allows concluding that optimal specific weight of light polystyrene concrete for ultralight steel concrete composite structures is 9 kN/m^3 with a strength under axial load 3500 kN/m^2.

4 Review of Analytical Model

One of the main tasks of the USCCS research is to solve the issue of local stability of their steel parts. Unlike traditional cold-formed structures, they rely on an elastic base, which is ultralight concrete. These elements should be considered as thin plates that come into contact with an elastic base, the modulus of elasticity of which is much smaller. This is a theoretical calculation model. At the same time, the stiffness of both components of the USCCS usually differs insignificantly.

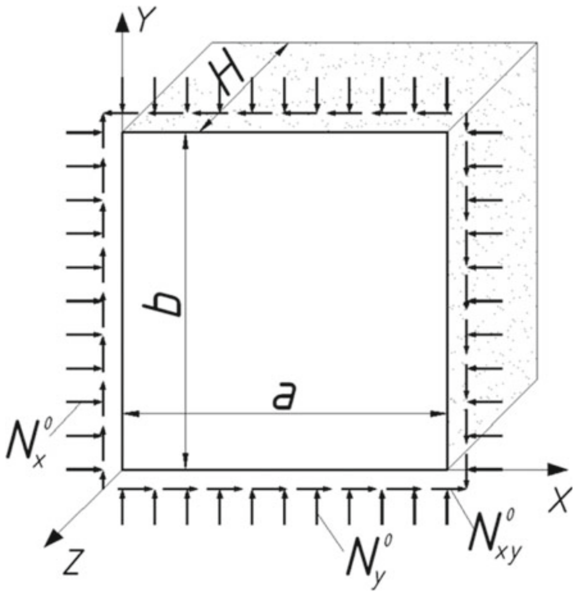

Fig. 4 The initial stress state of the plate, supported by an elastic base

Thus, the solution of the problem of local stability of steel elements of USCCS is reduced to the joint integration of the equations of the theory of shells and three-dimensional theory of elasticity, considering the boundary conditions on the contact surface of media (steel and concrete) and the conditions of these edges.

From this point of view, the rectangular steel plate is an integral part of the thin-walled rod and works in this direction in compression. The practical importance of the study of this necessitates the clarification of known engineering techniques [3], based on the analysis of methods for solving the basic equation of neutral equilibrium.

$$Z_0 = N_x^0 \omega_{xx} + 2N_{xy}^0 \omega_{xy} + N_y^0 \omega_{yy}. \tag{1}$$

Based on the assumption of a linear distribution of displacements in the thickness of the aggregate (ultralight polystyrene concrete), the equation of stability of a thin-walled steel plate on an elastic basis was considered by determining the specified relative to the deflection of the plate ω (Fig. 4).

$$K_1 K_2 L_1(\omega) - L_2(K_1 \omega_{xx} + K_2 \omega_{yy}) + \nabla_0^4 Q_z - \nabla_0^4 (N_x^0 \omega_{xx} + 2N_{xy}^0 \omega_{xy} + N_y^0 \omega_{yy}) = 0 \tag{2}$$

where L_1, L_2 are differential operators of shell theory, considering to account of the anisotropy of plates.

The most common cases of bearing capacity of the plate along the contour, compressed in one direction, with the corresponding boundary conditions of the

Table 1 Comparative analysis of theoretical and experimental bearing capacity of prototypes

Samples series	Load-bearing capacity, kN			
	Lightweight steel thin-walled structural elements			
	Experimental value	Theory of elasticity	Estimated value	Finite element
POF	2,40	3,04	3,34	3,02
POH	13,30	17,57	17,54	12,03
POR	48,00	42,96	37,52	36,40
	Lightweight composite steel and concrete structural elements			
PCF	27,00	–	28,23	27
PCH	34,00	–	52,34	45
PCR	92,00	–	74,87	68

unloaded sides were considered. It gives the division of such structures into lamellar elements.

From systems of homogeneous algebraic equations, considering the deformation of a plate with a rigidly bound elastic base, expressions were obtained to determine the critical load that is shown in Table 1, which was confirmed by experimental studies.

Hinged support:

$$N_{cr} = \min_{(k)}\left\{\frac{a^2 b}{k^2\pi^2}\left[F\left(\frac{k\pi}{a}, \frac{\pi}{b}\right) + q_{zk1}\right]\right\} \tag{3}$$

Fixed support:

$$N_{cr} = \frac{a^2 b}{3\pi^2}\min_{(k)}\left\{\frac{1}{k^2}\left[F_1\left(\frac{k\pi}{a}, \frac{2\pi}{b}\right) + 2q_{zk0} + 2q_{zk2}\right]\right\} \tag{4}$$

Free support:

$$N_{cr} = \min_{(k)}\left\{\frac{a^2 b}{k^2\pi^2}\left[F\left(\frac{k\pi}{a}\right) + q_{zk0}\right]\right\} \tag{5}$$

The critical load (N_{cr}) is the minimization of the right part of the expression with respect to $k = 1, 2, 3\ldots$, and the load function has the form:

$$\begin{aligned} F\left(\tfrac{k\pi}{a}, \tfrac{n\pi}{b}\right) &= \left[K_1\left(\tfrac{k\pi}{a}\right)^2 + K_2\left(\tfrac{n\pi}{b}\right)^2\right]\tfrac{\Delta_{kn}^{(1)}}{\Delta_{kn}^{(2)}} + K_2\varepsilon_2\tfrac{\Delta_{kn}}{\Delta_{kn}^{(2)}}; \\ F_1\left(\tfrac{k\pi}{a}, \tfrac{2\pi}{b}\right) &= \left[3K_1\left(\tfrac{k\pi}{a}\right)^2 + K_2\left(\tfrac{2\pi}{b}\right)^2\right]\tfrac{\Delta_k^{(3)}}{\Delta_k^{(4)}} + 3K_1\varepsilon_2\tfrac{\Delta_k^{(5)}}{\Delta_k^{(4)}}, \end{aligned} \tag{6}$$

where K_1, K_2 are the stiffness parameters that characterize the transverse displacements.

The value of the components is according to the following formulas, taking into account the compatible deformation of the plate with an elastic base:

$$\begin{aligned}
&\Delta_{kn} = \alpha_k^4 + 2(2\mu_1 + \nu_1)\alpha_k^2\beta_n^2 + \mu_{21}\beta_n^4;\quad \Delta_{kn}^{(1)} \\
&= \alpha_k^4 + (1 - \nu_1\nu_2 - 2\nu_2\mu_2)\alpha_k^2\beta_n^2 + \mu_1\beta_n^4; \\
&\Delta_{kn}^{(2)} = \Delta_{kn}^{(1)} + (\varepsilon_2 + \varepsilon_1\mu_2)\alpha_k^2 + (\varepsilon_1 + \varepsilon_2\mu_1)\beta_n^2 + \varepsilon_1\varepsilon_2; \\
&\Delta_{kn}^{(3)} = 3D_1D_3\left(\tfrac{k\pi}{a}\right)^4 + [(3 - \upsilon_1\upsilon_2)D_2 - 2\upsilon_2D_3]D_1\left(\tfrac{2k\pi^2}{ab}\right) + D_2D_3\left(\tfrac{2\pi}{b}\right)^4; \\
&\Delta_{kn}^{(4)} = \Delta_{kn}^{(3)} + 3(D_1K_2 + D_3K_1)\left(\tfrac{k\pi}{a}\right)^2 + (D_3K_2 + 3D_2K_1)\left(\tfrac{2\pi}{a}\right)^2 + 3K_1K_2; \\
&\Delta_{kn}^{(5)} = 3D_1\left(\tfrac{k\pi}{a}\right)^4 + 2(\upsilon_2D_1 + D_3)\left(\tfrac{2k\pi^2}{ab}\right) + D_2\left(\tfrac{2\pi}{b}\right)^4,
\end{aligned} \tag{7}$$

where, the isotropy of the plate is taken into account:

$$\mu_1 = \frac{G\left(1 - \nu^2\right)}{E}, \tag{8}$$

where D_1 is the cylindrical stiffness of the plate; ν and E are the Poisson's ratio and the modulus of elasticity of the plate material; α and β are the parameters of the plate formation wave; q_{zkn} - component that takes into account the reaction of the elastic filler.

$$q_z = 2G_c\sqrt{\alpha^2 + \beta^2}\,\frac{f_1 + \chi g_1}{f_2 + \chi g_2}, \tag{9}$$

where G_c is the shear modulus of the elastic base; ν_c and E_c - Poisson's ratio and modulus of elasticity of the base material.

$$\begin{aligned}
&f = (1 - 2\nu c)sh^2\eta * + \gamma_+\gamma_- H^2 + 2(1 - \nu_c)(1 - 2\nu c)\left(1 - \gamma_+/\gamma_-\right); \\
&f_1 = (1 - \nu c)(sh2\eta * - 2\gamma_- H); \\
&f_2 = (3 - 4\nu c)ch^2\eta * + \gamma_+\gamma_- H^2 + (1 - 2\nu c)\left[3 - 4\nu c - 2(1 - \nu c)\gamma_+/\gamma_-\right]; \\
&g_1 = sh^2\eta * - \gamma_+\gamma_- H^2 + 2(1 - \nu c)(1 - 2\nu c)\left(\gamma_+/\gamma_- + \gamma_-/\gamma_+ - 2\right); \\
&g_2 = (1 - \nu c)(sh2\eta * + 2\gamma_- H); \\
&\chi = -2Gc\frac{2\alpha\beta d_{xy} - \alpha^2 d_x - \beta^2 d_y + 2Gc\gamma_+^3 th\,\eta *}{B\gamma_+^2 d_{\alpha\beta} - Gc\left(2\alpha\beta d_{xy} + \alpha^2 d_y + \beta^2 d_x\right)\gamma_+ th\,\eta *}.
\end{aligned} \tag{10}$$

Thus, the problem is reduced to the iterative refinement of expressions (3)–(5), that is the reduction of bearing capacity depending on the nature of the waveform k, n.

Using the obtained dependences to determine the influence of the properties of the reinforcing base, the dependences of the interaction N (ν, E) were considered. The modulus of elasticity E_s and the Poisson's ratio ν_s varied from 1000 MPa to 100,000 MPa and 0.1… 0.3, respectively, which is covered a significant number of physical and mechanical properties of concrete.

A decrease in critical forces is initially observed in the case of a three-layer structural element for a filler with a very low modulus of elasticity E_s at low H. This is due to the large shear deformations of the aggregate, which reduce the bending stiffness of the wall so much that it becomes less than the stiffness of the bearing layers (the stiffness of the walls at $H = 0$). In fact, with very small E_c modules, the load-bearing layers operate almost independently of each other when the stability is lost.

Meanwhile, it is physically clear that critical efforts must continue to grow. The results of the solutions show that this increase at low modulus of elasticity of the aggregate is very small, because the parts of the aggregate, far enough from the carrier layers, do not have a supporting effect on the latter from each other.

Under different conditions of fixing the unloaded edges of a rectangular plate with a thickness of 1 mm, the obtained dependences are curvilinear. It consists of increasing modulus of elasticity increases the load-bearing capacity of the structural element, and increasing the value of ν_s, in turn, does not significantly reduce the value of N. ν. It (ν) can be significant for structures whose layers are orthotropic and have very different Poisson's ratios.

Based on the condition that the greater strength of concrete significantly increases the stability not only of thin-walled elements of reinforced concrete structures, but also perceives considerable effort, which is not always justified. Because under such conditions the weight of the structure increases significantly, Poisson's ratio ν_s was taken as 0,15, modulus of elasticity $E_s = 5000$ MPa, as the physical and mechanical characteristics that best correspond to lightweight concretes. It is used in subsequent experimental studies (Fig. 5).

A detailed analysis revealed that at relatively large values of H (0.1… 0.3 and more), which exceed the geometric dimensions of the plate, remote parts of the aggregate do not have a supportive effect. It indicates irrational use of elastic base material at certain limits conditions and sizes, regardless of the selected material of reinforcing base.

The main task of experimental research was to obtain quantitative and qualitative data on the influence of steel elements thickness and concrete composition of reinforced concrete structures on local stability and stress–strain state of compressed steel and reinforced concrete structures under static load, also with their bearing capacity and fracture nature.

Modeling of light steel thin-walled plates (PO) and light thin-walled reinforced concrete elements (PC) in software complexes by the finite element method allowed to take into account the features of loss of stability of thin-walled steel plate and to investigate their work in more detail.

Different boundary conditions were applied to the corresponding faces of thin-walled steel plates to bring the models as close as possible with the help of a software package. It consists of free edges (POF, PCF), hinged support (POH, PCH), and rigid clamping (POR, PCR) of unloaded sides.

An additional layer of two-dimensional orthotropic material with a thickness of 0.1 mm was introduced to model the reaction properties of the elastic base in conjunction with the steel component of the structure. This approach allowed obtaining and

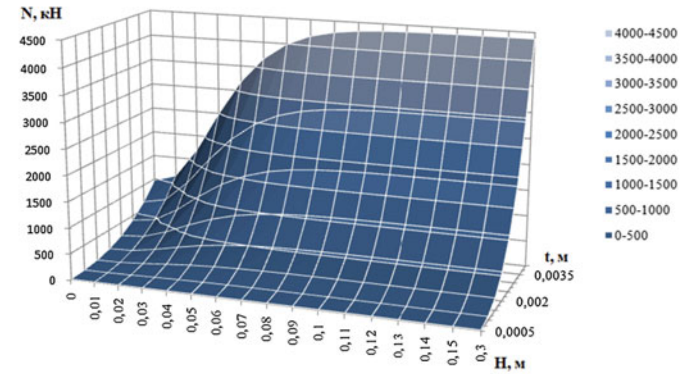

(a) Hinged support

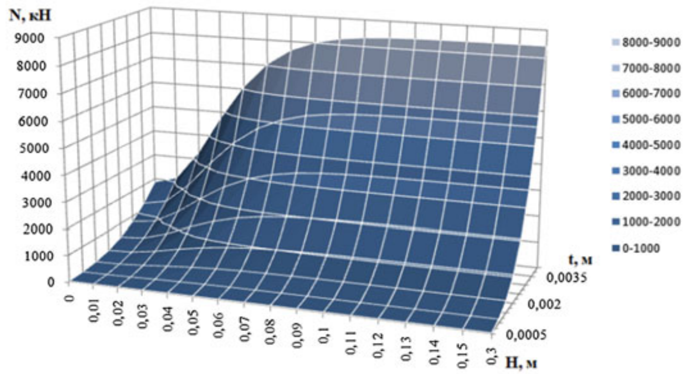

(b) Fixed support

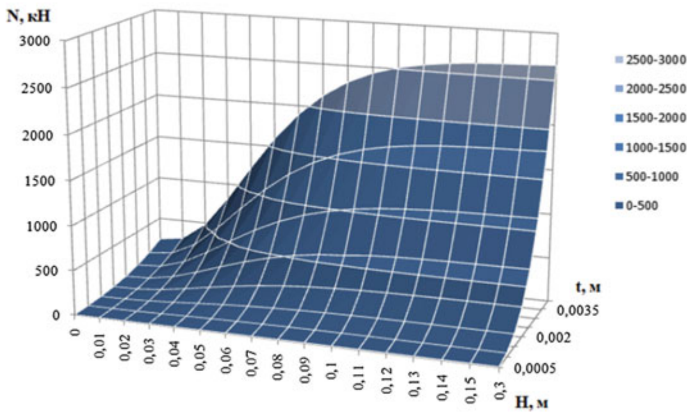

(c) Free support

Fig. 5 Interaction surfaces N (νs, Es) under different boundary conditions of longitudinal unloaded sides.

varying the amount of "gluing" of concrete to the plate, and as a result, it is the actual work of the structure.

As a result of finite element calculations using a computer "Destruction" of the sample models is as follows: the sample with a hinged support of the steel plate along the contour is formed by one half-wave in the transverse and longitudinal directions at a critical load of 45 kN. In the model, which is a reinforced concrete structural element with rigid clamping of the unloaded sides of the steel plate - two half-waves in the longitudinal direction and one in the transverse at a value of 68 kN. And one half-wave in the longitudinal direction at 26.7 kN with free support.

5 Conclusions

Therefore, as expected by theoretical calculations, despite the relatively small modulus of elasticity of the reinforcing base (lightweight concrete), the bearing capacity of the samples increases significantly, which indicates the feasibility of lightweight concrete component in lightweight steel structures to prevent local loss of stability.

The difference between the critical experimental and theoretical load for the samples of the series of POF and PCF was not more than 8.9%; for samples of the POR and PCR series about 14%, because in the theoretical calculation insignificant stiffening ribs were not taken into account for modeling the clamping of the longitudinal sides. The significant difference in the critical load for the samples of the POH and PCH series that is due to experimental studies, because it is quite difficult to obtain an ideal hinge. It is obvious that for samples with a concrete component this deviation is smaller.

References

1. ANSYS (2011). User's manual revision 14.0. Canonsburg, PA: ANSYS, Inc.
2. Bock M, Real E (2015) Effective width equations accounting for element interaction for cold-formed stainless steel square and rectangular hollow sections. Structures 2(2015):81–90
3. EN 1994–1–1 (2004). Eurocode 4: design of composite concrete and steel structures – part 1–1: general rules and rules for buildings. Brussels: European Committee for Standardization (CEN)
4. EN 1993–1–3 (2006). Eurocode 3: design of steel structures. Part 1–3: General rules. Supplementary rules for cold-formed members and sheeting. Brussels: European Committee for Standardization (CEN)
5. Ewadh HM, Basri NA (2012) Effectiveness of polystyrene beads as aggregate replacement material to recycle solid waste: a study on workability and absorption results of concrete. Int J Sci Eng Res 3(8):1–4
6. Liew JYR, Koh CG, Sohel KMA (2009) Impact tests on steel-concrete-steel sandwich beams with lightweight concrete core. Eng Struct 31(9):2045–2059
7. Park SG, Chisholm DH (1999) Polystyrene aggregate concrete. Study Report. SR 85, Building Research Association of New Zealand, Judgeford

8. Shanmugam NE, Kumar G (2002) Thevendran V (2002) Finite element modelling of double skin composite slabs. Finite Elements Anal Des 38(7):579–599
9. Tamut T, Prabhu R, Venkataramana K, Yaragal SC (2014) Partial replacement of coarse aggregates by expanded polystyrene bead in concrete. Int J Res Eng Technol 03(02):238–241
10. Leshchenko MV, Semko V (2015) Thermal characteristics of the external walling made of cold-formed steel studs and polystyrene concrete. Mag Civil Eng 60(8):44–55
11. Hasenko A, Semko O, Drobotia O, Sirobaba V (2020) Experimental and numerical studies of nodes of light steel-reinforced concrete structures. In: Paper presented at the Proceedings of the 2020 Session of the 13th Fib International PhD Symposium in Civil Engineering, pp 73–178
12. Onischenko VA, Soloviev VV, Chernenko LA, Malyshev VV, Bondus SN (2014) Acidic-basic interactions in tungstate melts based on tungsten electroplating out of them. Materialwissenschaft Und Werkstofftechnik 45(11):1030–1038. https://doi.org/10.1002/mawe.201400222
13. Kochkarev D, Azizov T, Galinska T (2018) Bending deflection reinforced concrete elements determination. Paper presented at the MATEC Web of Conferences, p 230. https://doi.org/10.1051/matecconf/201823002012
14. Pichugin SF (2018) Reliability estimation of industrial building structures. Mag Civil Eng 83(7):24–37. https://doi.org/10.18720/MCE.83.3
15. Zotsenko M, Vynnykov Y, Lartseva I, Sivitska S (2018) Ground base deformation by circular plate peculiarities. In: Paper presented at the MATEC Web of Conferences, p 230. https://doi.org/10.1051/matecconf/201823002040
16. Cherniha R, Pliukhin O (2013) New conditional symmetries and exact solutions of reaction-diffusion-convection equations with exponential nonlinearities. J Math Anal Appl 403(1):23–37. https://doi.org/10.1016/j.jmaa.2013.02.010